Appl. Phys. A 59, 135–138 (1994)

Applied Physics A Solids and Surfaces

Selective imaging of self-assembled monolayers by tunneling microscopy

J. P. Bucher, L. Santesson*, K. Kern

Institut de Physique Expérimentale, EPF Lausanne, CH-1015 Lausanne, Switzerland
(Fax: +41-21/693-3604)

Received 18 January 1994/Accepted 24 March 1994

Abstract. The properties of thin organic films offer many challenging opportunities for science and technology. A crucial requirement for the advancement of molecular film technology is the selective characterization and modification on an atomic level. Local proximal probes like Scanning Tunneling Microscopy (STM) or Atomic Force Microscopy (AFM) bear certainly the potential for this purpose. So far, however, mainly adsorbed organic molecules lying flat on a smooth substrate have been imaged with near atomic resolution. Here, we demonstrate the ability of STM to selectively image self-assembled monolayers of long-chain molecules (hexanethiol) oriented upright on the substrate Au(111) with molecular resolution. Upon proper choice of the tunneling parameters we can image the molecular head-group anchored at the substrate and/or the molecular tail group.

PACS: 68.55,61.16.Ch

A particular promising method for the controlled formation of thin organic films is the self-assembly technique [1]. Compared to the sophisticated Lagmuir-Blodgett technique [2], the self-assembly process is characterized by its ease of operation and the non-restricted sample geometry. In particular the ω-functionalized long-chain alkanethiols have been found to form highly ordered and stable Self-Assembled Monolayers (SAMs) on noble-metal substrates [3]. While the sulfur head-group assures, via a strong covalent bonding to the substrate, high mechanical and thermal stability, the tail-group serves for functionalization purposes to control the interfacial properties of the monolayer. On Au(111) numerous studies have revealed the characteristic brush-like ordering (Fig. 1a) of the alkanethiols [3]. The alkyl chains are ordered in a high-density crystal-like packing with the sulfur head group adopting a $(\sqrt{3} \times \sqrt{3})R30°$ structure (Fig. 1b). The chains are in all-trans conformation with an average tilt of $\alpha \approx 30°$ of the molecular axes from the surface normal.

Recent structural studies of the self-assembled alkanethiols did, however, reveal the presence of a high density of defects in the monolayer [4–6]. In thermal helium- and *X*-ray-diffraction a substantial diffraction peak broadening was noticed indicating a coherence length of less than 100Å [4]. This behavior was associated with the pressence of domain boundaries separating neighboring anti-phase $\sqrt{3}$ domains. In addition, STM [5] and AFM [6] images revealed the presence of small depressions (1–3 nm in diameter) randomly distributed in the molecular film. The nature of the holes was a matter of controversial discussion. The explanations which have been put forward include electronic artifacts of the STM [6], the accumulation of "gauche" defects within the thiol layer [7] and defects in the topmost gold substrate layer [5].

The substrate origin of the defects has recently convincingly been demonstrated by studying their thermal evolution with STM [8, 9]. The substrate holes are formed during the self-assembly process via chemical erosion of gold atoms and are confined to the first substrate layer. In our in-situ STM [8] study the substrate holes have been found to migrate and coalesce to large vacancy islands upon thermal annealing. These vacancy islands, several 10 nm in size, exhibit a characteristic quasi-triangular equilibrium shape, characteristic for vacancy islands within a fcc(111) surface [8, 10]. In Fig. 1c, d we demonstrate that the thermal mass transport can be used to order the hexanethiol/gold interface. Upon extensive annealing at 350 K the vacancy islands diffuse towards preexisting substrate steps where they are annihilated leaving perfectly flat depression-free SAMs.

The STM experiments shown in Fig. 1 and reported below have been done with a home-built "beetle-type" microscope. Due to its inherent thermal self-compensation, this microscope is particularly suited vor variable temperature studies. For UHV applications we have recently developed a system for a sample temperature

* Present address: Institut de Physique Appliquée, Université de Genève, CH-1211 Genève, Switzerland

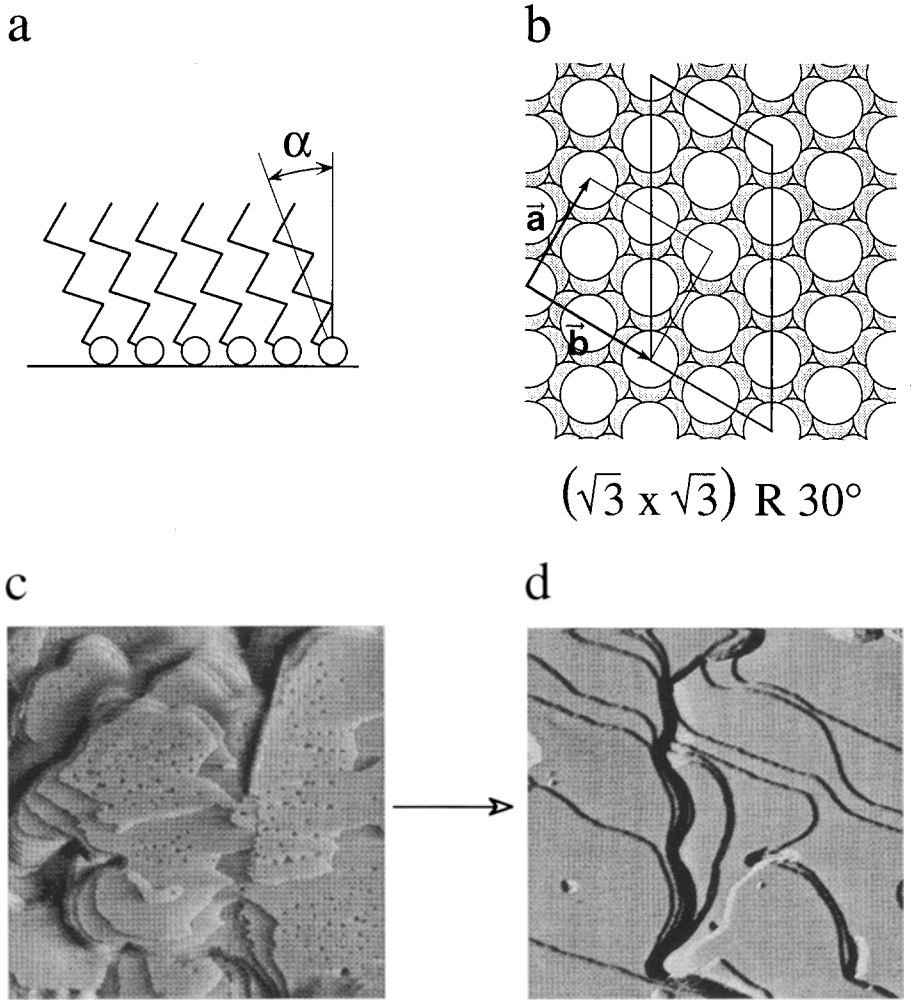

Fig. 1a–d. Molecular arrangement and morphology of the thiol/Au(111) interface. **a** Schematic side view of a self-assembled alkanethiol monolayer on a Au(111) substrate. **b** Plane view of the lateral $(\sqrt{3}\times\sqrt{3})R30°$ ordering of the sulfur headgroups on Au(111). The unit cell of a $c(4\times2)$ superstructure and the corresponding unit vectors **a** and **b** oriented along the $<1,-1,0>_{Au}$ and $<1,1,-2>_{Au}$ direction, respectively, are also indicated. **c** STM image of hexanethiol monolayer on Au(111), 480 nm × 480 nm. Self-assembly and imaging at 300 K. **d** STM image of the same hexanethiol monolayer after extensive annealing at 350 K, 480 nm × 480 nm

range from 25 K to 800 K [11]. In the present application for the study of organic monolayers in liquids or in ambient atmospheres a temperature variability from 250 K to 400 K is obtained by coupling the sample to a Peltier element [12]. As substrates we used Au(111) films epitaxially grown on mica in ultrahigh vacuum. The gold films were flame-annealed in an butane-oxygen flame and quenched in ethanol. After a second flame annealing, SAMs of hexanethiol were prepared by dipping the substrate in a 1 mM hexanethiol solution of ethanol (dipping times ranging from several minutes to several hours) and final rinsing in ethanol. Quality control of substrates and organic films has been performed by Auger-electron spectroscopy and infrared spectroscopy. The STM images in Fig. 1 were recorded in differential mode, which means that the derivative of the lines of constant tunnel current is recorded, whereas Figs. 2 and 3 show STM images with the grey-scale (false-color scale) representing the absolut tip height.

In Fig. 2 we compare a high-resolution STM image of the self-assembled hexanethiol monolayer with the atomically resolved STM image of the clean Au(111) substrate (inset). In both images a hexagonal close-packed pattern of bright spots is observed. The comparison of the hexanethiol STM image with the image of the clean Au(111) surface reveals an increased nearest neighbor distance of the molecular lattice, measured to be 4.98Å (which has to be compared to the Au(111) lattice parameter of 2.88Å). In addition, the monolayer unit cell is rotated by 30° with respect to that of the substrate. Both observations are in perfect-agreement with the $(\sqrt{3}\times\sqrt{3})R30°$ structure found to be adopted by the sulfur head group on the Au(111) substrate [3]. We might thus identify the spots in the STM image with the position of the sulfur atoms. Recent STM studies of sulfur adsorption on a Re(0001) surface in ultrahigh vacuum do indeed show a very similar contrast arising from the sulfur-rehnium bond [14]. The image contrast in Fig. 2 is thus believed to be dominated by tunneling via the gold bound sulfur head group of the hexanethiol. The alkyl chain and the methyl tail-group seem to have a negligible influence under the applied tunneling conditions. Information on the actual registry (i.e., identification of the adsorption site) of the sulfur head groups could, however, not be obtained, any attempts to image the substrate in the presence of the organic monolayer have failed so far. For convenience we assume the fcc hollow site as energetically preferred adsorption site.

Recent experiments on Langmuir-Blodgett films indicate, however, that under certain tunneling conditions

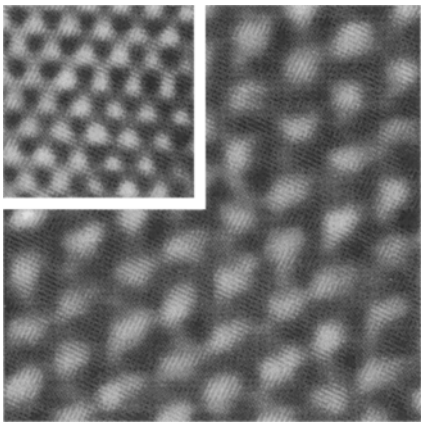

$S\ (\sqrt{3} \times \sqrt{3})\ R\ 30°$

Fig. 2. STM images of the self-assembled hexanethiol monolayer, 3.4 nm × 3.4 nm, I = 1.0 nA, U = 0,5 V. Inset: the clean Au(111) substrate I = 32 nA, U = 10 mV

also a contrast contribution from the alkyl chains or from the tail-groups might be expected [15]. To be more sensitive to the outer interface of the hexanethiol monolayer we have measured constant current topographs with increasing tunneling voltage; i.e., we are sampling the monolayer at larger distance from the substrate. In Fig. 3a we show an example obtained with 0.72 V. Surprisingly the image does exhibit now a rectangular symmetry rather than the hexagonal symmetry of Fig. 2. The rectangular unit cell has unit vectors of 9.9Å length along the $<1,1,-2>_{Au}$ direction and 8.6 Å length along the $<1,-1,0>_{Au}$ direction.

The observation of this rectangular pattern with a unit mesh of dimensions 9.9Å × 8.6Å in the STM image is in perfect agreement with recent He-diffraction data of Camillone et al. [16]. These authors have performed He-diffraction measurements from self-assembled alkanethiols on Au(111) and observed superlatice diffraction peaks, which they assigned to a $c(4 \times 2)$ superstructure with unit vectors of 10.02Å and 8.68Å (see Figs. 1 and 8 in [16]). Due to its thermal energy (14 meV) the probing He beam does not penetrate the thiol monolayer. He diffraction is exclusively sensitive to the ordering of the outermost part of the molecular layer, i.e., the tail-groups, and Camillone et al. proposed that the $c(4 \times 2)$ unit mesh has to be the result of a patterned arrangement of rotations of the methyl tail groups (or rotations of the whole alkyl chains about their molecular axes). The authors suggest two possible unit cell models, the first in which one chain is twisted clockwise and three chains are twisted counterclockwise and the second unit mesh, where two chains are twisted clockwise and two chains are twisted counterclockwise. In both cases the geometric height difference of the terminal methyl-groups generated by the twist configuration of the tilted chains is thought to be responsible for the observation of the superstructure in He diffraction. From the fact that we observe the same rectangular super-cell in our STM image Fig. 3a we conclude that the STM contrast in this image is dominated by tunneling through the "twist-patterned" tail-groups.

More detailed information on the physical origin of the $c(4 \times 2)$ pattern in our STM images can be drawn from a close inspection of Fig. 3b. In this false-color image (30Å × 30Å) taken at a tunneling voltage of 1.0 V a complex contrast composed of the $(\sqrt{3} \times \sqrt{3})R30°$ sulfur pattern (yellow spots) and the $c(4 \times 2)$ tail-group pattern (white spots) is observed. The positions of the bright $c(4 \times 2)$ spots do not fully coincide with the mesh of the $\sqrt{3}$ structure. The center of the bright spots is slightly displaced ($\approx$1Å) towards the direction of the next-nearest sulfur neighbor. This effect might be explained if we assume that the tunneling contrast is a superposition of the tunneling through the gold-sulfur bond and the tunneling through the molecular tail. Due to the tilt of the alkyl chain with respect to the surface normal the projection of the methyl tail-group onto the surface does not coincide with the position of the sulfur-head atom. For the alkanenethiols on Au(111) the average tilt angle has been measured to be $\approx 30°$. Hence, the projected center of the methyl-group is displaced by 3.3Å from the sulfur position. Depending on the weight of the tunneling probabilities of head- and tail-group the STM image will show its maximum height somewhere on the axis between the sulfur position and the projected tail-group position. From the STM image in Fig. 3b we can thus determine the molecular tilt direction along the $<1,-1,0>_{Au}$ azimuth. This tilt direction is in perfect accord with recent

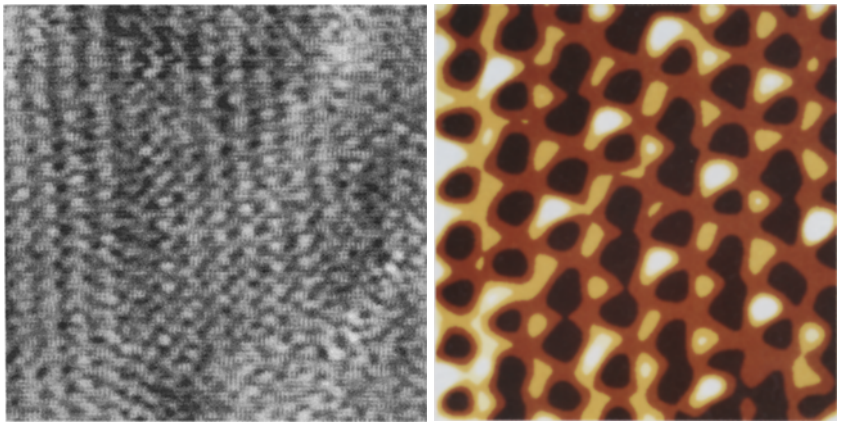

Fig. 3a, b. STM images of the hexanethiol monolayer acquired at different sampling heights. **a** 15 nm × 15 nm, I = 1.0 nA, U = 0.72 V. **b** 3.4 nm × 3.4 nm, I = 1.2 nA, U = 1.0 V; in the false-color scale red corresponds to the lowest and white to the largest height (red→orange→yellow→white)

X-ray diffraction measurements [17]. The actual $c(4 \times 2)$ structure seen in the STM images, however, is not in accord with the two "twist-ordering" models suggested by Camillone et al. [16]. A superstructure consistent with the STM images would be for instance a pinwheel structure with the central atom twisted counterclockwise and the surrounding six atoms twisted clockwise.

The STM image contrast of semiinsulating molecules on conducting substrates, in first approximation, arises from the adsorbate induced modifications of the substrate tunneling current. This modification has mainly two contributions, the change in barrier height (i.e., the change of the local work function) [18] and/or the change in the electronic density of states [19]. This approach has been applied with some success in the interpretation of the image contrast of flat lying organic molecules. The tunneling mechanism resulting in the enhanced tail-group contrast in the STM-images shown in Fig. 3, however, is not readily explainable in this simple picture. The typical STM current of 1 nA corresponds to about 10^{10} electrons per second, which is five orders of magnitude higher than the expected electrical conductivity of the hexanethiol molecule [20]. Several models have been offered, in order to explain the measured large tunneling currents through alkyl chains including the injection of electrons into loosely bound nonlocalized orbitals [21], electron conductance by hopping [22] or resonant tunneling [23].

In the present case of hexanethiol monolayers on Au(111) the situation is even more complex as elastic tip-molecule interactions seem to play a decisive role in the image contrast formation. The simultaneous appearence of the $c(4 \times 2)$ and the $(\sqrt{3} \times \sqrt{3})R30°$ pattern is depending on the actual scan direction. In Fig. 3b with both patterns present the scan direction was oriented 60° off the molecular tilt plane. Upon rotation of the scan direction by 60°, i.e., orienting the scan direction along the plane of the molecular tilt of the hexanethiol molecules, the complex image contrast vanishes and only a regular $(\sqrt{3} \times \sqrt{3})R30°$ pattern is observed under otherwise identical tunneling conditions.

The further advancement in the understanding of STM images of SAMs certainly implies the development of sophisticated theoretical image simulations, following for example the ideas of Sautet et al. [14]. Such STM simulations of adsorbed organic layers should, however, not only account for the proper morphology and chemical identity of the tip and the sample and the details of the electronic wave functions in the gap region but must also include the elastic interactions between the tip and the sample. The hexanethiol monolayer on gold with its complex contrast behavior might be the ideal model system to develop the appropriate theoretical tools.

The present work bears two implications of general importance. Firstly, defects at the thiol/gold interface can be healed out upon gentle annealing, without affecting the overall structure of the monolayer. Secondly, by appropriate choice of the tunneling parameters the molecular arrangement of the substrate-anchored head-group and/or the interfacial tail-group can be imaged selectively. The latter point is of particular importance. For most applications of SAMs it is the structure and orientation of the tail functional group which is of importance. This is the part of the molecules that dominates the interaction between the monolayer and a contacting phase. Tunneling microscopy can thus provide a molecular view of interfacial SAM phenomena like adhesion, chemical processing, molecular recognition etc.

Acknowledgement. This research has been supported by the Schweizerischer Nationalfonds.

References

1. A. Ullmann: *An Introduction to Ultrathin Films* (Academic, New York 1991)
2. K.B. Blodgett: Am. Chem. Soc. **57,** 1007 (1935)
3. L.H. Dubois, R.G. Nuzzo: Annu. Rev. Phys. Chem. **43,** 437 (1992)
4. N. Camillione, C. Chidsey, P. Eisenberger, P. Fenter, J. Li, K.S. Liang, G.Y. Liu, G.J. Scoles: Chem. Phys. **74,** 744 (1993)
5. K. Edinger, A. Gölzhäuser, K. Demota, C. Wöll, M. Grunze: Langmuir **9, 4** (1993)
6. D. Anselmetti, Ch. Gerber, B. Michel, H. Wolf, H.-J. Güntherodt, H. Rohrer: Europhys. Lett. **23,** 421 (1993)
7. U. Dürig, B. Züger, B. Michel, L. Häussling, H. Ringsdorf: Phys. Rev. B **48,** 1711 (1993)
8. J.-P. Bucher, L. Santesson, L. Kern: Langmuir **10,** 979 (1994)
9. R.L. McCarley, D.J. Dunaway, R.J. Willicut: Langmuir **9,** 2775 (1993)
10. Th. Michely, K.-H. Besocke, G. Comsa: Surf. Sci. **230,** L135 (1990) Th. Michely, G. Comsa: Surf. Sci. **256,** 217 (1991)
11. H. Röder, H. Brune, J.P. Bucher, K. Kern: Surf. Sci. **298,** 121 (1993) H. Röder, E. Hahn, H. Brune, J.P. Bucher, K. Kern: Nature **366,** 141 (1993)
12. J.P. Bucher, H. Röder, K. Kern: Surf. Sci. **289,** 370 (1993)
13. C.A. Widrig, C.A. Alves, M.D. Porter: J. Am. Chem. Soc. **113,** 2805 (1991)
14. J.C. Dunphy, D.F. Ogletree, M.B. Salmeron, P. Sautet, M.L. Bocquet, C. Joachim: Ultramicroscopy **42–44,** 490 (1992)
15. D.P. Smith, A. Bryant, C.F. Quate, J.P. Rabe, G. Gerber, J.D. Swalen: Proc. Natl. Acad. Sci. USA **84,** 969 (1987)
16. N. Camillone, C. Chidsey, G.Y. Liu, G. Scoles: J. Chem. Phys. **98,** 3503 (1993)
17. P. Fenter: (in press)
18. J.K. Spong, H.A. Minzes, L.J. LaComb, M.M. Dovek, J.E. Frommer, J.S. Foster: Nature **338,** 137 (1989)
19. H. Ohtani, R.J. Wilson, S. Ching, C.M. Mate: Phys. Rev. Lett. **60,** 2398 (1988)
20. C. Chidsey: Science **251,** 919 (1991)
21. J. Hörber, C.A. Lang, T.W. Hänsch, W.M. Heckl, H. Möhwald: Chem. Phys. Lett. **145,** 151 (1988)
22. W. Mizutani, M. Shigeno, K. Saito, K. Watanabe, S. Sugi, M. Ono, K. Kajimura: Jpn. J. Appl. Phys. **27,** 1803 (1988)
23. B. Michel, G. Travaglini, H. Rohrer, C. Joachim, M. Amrein: Z. Phys. B **76,** 99 (1989)